


RESEARCH ARTICLE

The east–west division of changing precipitation in Nepal

Binod Pokharel^{1,2}  | S.-Y. Simon Wang^{1,2} | Jonathan Meyer^{1,2} |
Suresh Marahatta³ | Bikash Nepal⁴ | Yoshimitsu Chikamoto² | Robert Gillies^{1,2}

¹Utah Climate Center, Utah State University, Logan, Utah

²Department of Plants, Soils, and Climate, Utah State University, Logan, Utah

³Central Department of Hydrology and Meteorology, Thibhuvan University, Kathmandu, Nepal

⁴Department of Hydrology and Meteorology, Government of Nepal, Kathmandu, Nepal

Correspondence

Binod Pokharel, Utah Climate Center, Department of Plants, Soils, and Climate, Utah State University, Logan, UT.
Email: binod.pokharel@usu.edu

Funding information

Utah State University Agricultural Experiment Station; U.S. Department of Energy

Abstract

Changes to precipitation patterns and extremes over the Nepalese Himalayas were examined using a high-resolution, station-based daily dataset, Asian Precipitation-Highly Resolved Observational Data Integration Towards Evaluation (0.05° × 0.05° APHRODITE) from 1951 to 2007. The annual statistics of extreme precipitation across Nepal show a significant increase since the end of the 20th century. However, seasonal mean precipitation shows a remarkable decrease in western Nepal, particularly since 1980, forming an east–west division in the precipitation change. This decreasing trend of precipitation led to a reduction to the dry-season stream flow of Karnali River, the major river in western Nepal. At the same time, the increasing extreme precipitation produced greater threat of flash flood in Nepal. This east–west division of the precipitation trend agrees with the second leading mode of the mean precipitation variability, which was traced to the interannual variability of the Indian Ocean sea surface temperature that showed a slowdown of warming. Similar to the APHRODITE trends, precipitation simulated by the fifth phase of the Coupled Model Intercomparison Project (CMIP5) models depicted the decreasing historical trend in western Nepal, but future projections reverse that trend towards an all-Nepal increase. CMIP5 future climate projections depict continual warming in the Indian Ocean, potentially reversing the historical decreasing trends of precipitation in western Nepal.

KEYWORDS

extreme precipitation, changing precipitation Nepal

1 | INTRODUCTION

The Himalayan region is warming faster than the rest of the globe and this warming has been accompanied by an increase of extreme weather events (Krishnan *et al.*, 2019). In addition to the known risk of increased extreme precipitation in the lower elevation, the warmer atmosphere acts to increase total precipitation over tall mountains while decreasing snowfall (Viste and Sorteberg, 2015), hence enhancing the risk for glacier lake outburst. While the Indian summer monsoon from June to September contributes to the majority (~80%) of annual

precipitation in Nepal, the remaining 20% of annual precipitation received during the other 8 months has significant impacts on agriculture. Geographically, western Nepal receives less annual precipitation than central and eastern Nepal and therefore responds more profoundly to precipitation change (Wang *et al.*, 2013). The decreasing precipitation trend in Western Nepal poses a threat to the people, agriculture, ecosystems, and economy (Adhikari, 2019; Sudmeier-Rieux *et al.*, 2012).

During the last three decades, precipitation associated with the summer monsoon over the Indian subcontinent has seen a significant change (Roxy *et al.*, 2015; Jin and

Wang, 2017). However, the change in the Indian precipitation pattern does not necessarily reflect the precipitation change in Nepal. Topography plays a major role on the spatial distribution of precipitation with increasing magnitude up to the southern mountain ranges (called the Churia range) where warm and moist monsoonal air is orographically lifted (Kansakar *et al.*, 2004). Analysis of high-resolution gridded precipitation data indicates that Western Nepal has experienced a significant decrease in precipitation

during recent years, while most part of the eastern region shows increasing precipitation trend (Figure 1; to be discussed later).

Despite the recent examination in extreme precipitation (Bohlinger and Sorteberg, 2017; Karki *et al.*, 2017; Talchabhadel *et al.*, 2018), Nepal does not yet have reliable weather forecasting and early warning systems and its rainfall measurements are limited and sparse. Previous extreme precipitation studies have mostly used either station data (Bohlinger and Sorteberg, 2017; Karki *et al.*,

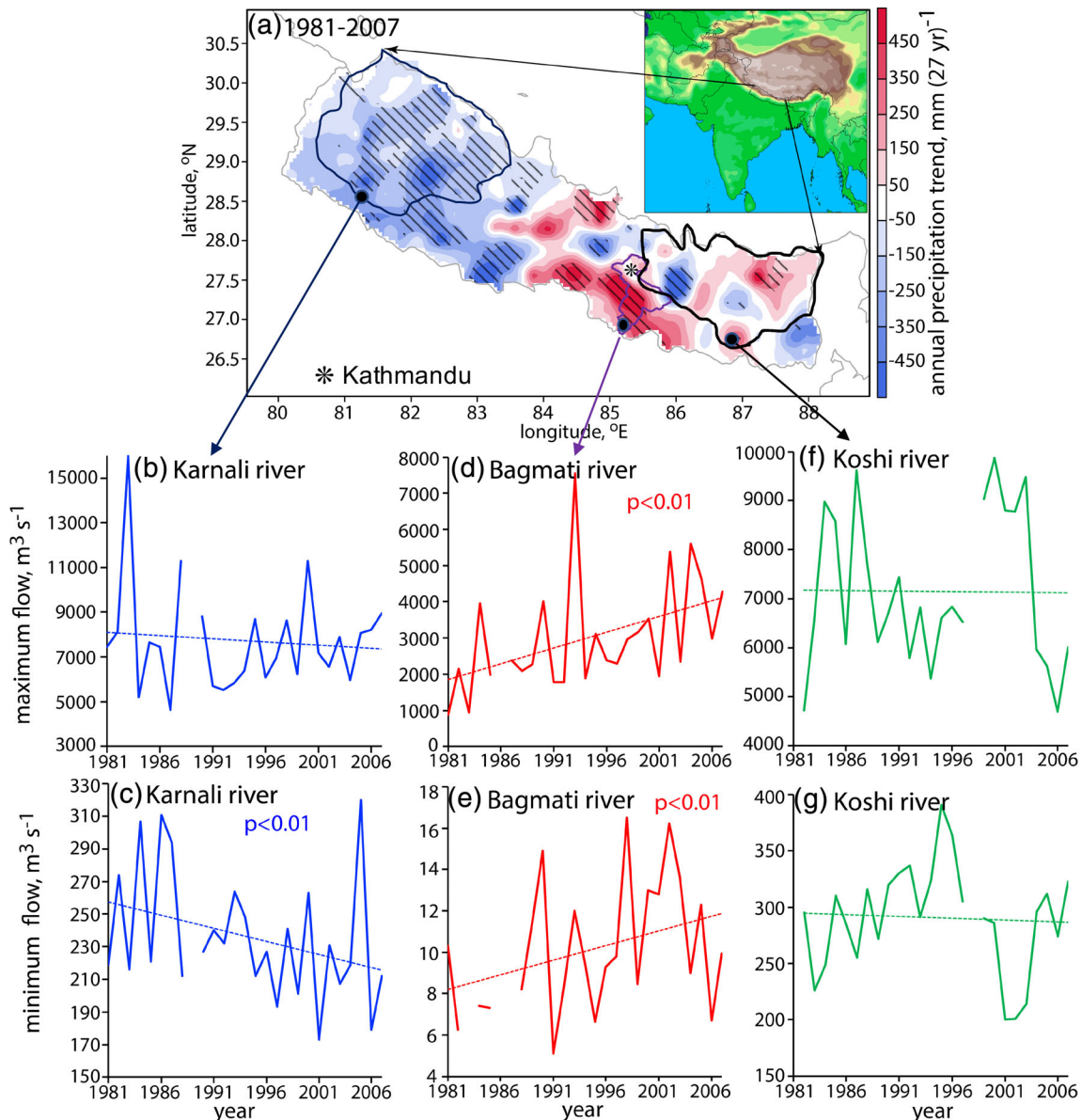


FIGURE 1 Annual precipitation trend from 1981 to 2007 in Nepal using 5 km resolution APHRODITE data. (a) Linear trend of annual precipitation in 27 years and hatched areas indicate significant values with $p < .05$. (b) and (c) show the maximum and minimum flow of Karnali River, respectively. Similarly, (d) and (e), and (f) and (g) show maximum and minimum flow of Bagmati and Koshi rivers. Dashed line from (b) to (g) shows the linear trend and p -value is given if there is any significance. Basin boundary and flow measurement locations are given in (a). All data are shown only after 1980 and gap in time series plots indicates that no measurements are available for that particular year. The flow of Karnali, Bagmati, and Koshi Rivers are measured at Chisapani, Padhera Dovan, and Chatara, respectively, and all three rivers originate on the north and flowing to south [Colour figure can be viewed at wileyonlinelibrary.com]

2017; Bohlinger *et al.*, 2018; Talchabhadel *et al.*, 2018), satellites, and/or coarse-resolution gridded data (Houze *et al.*, 2007; Baidya *et al.*, 2008; Romatschke *et al.*, 2010; Romatschke and Houze, 2011). While remote sensing measurements are commonly used to supplement surface observations, most of these platforms either underestimate the amount or misrepresent the location (Palazzi *et al.*, 2013). The majority of extreme precipitation in Nepal occurs in highly localized areas, which can make quantifying the precipitation extremes difficult if that region does not have any measurements.

To focus on the spatial pattern of extreme precipitation, we used a high-resolution precipitation data set that has not been utilized in these previous studies. A description of the data sets used in this study and the methodology is provided in Section 2. Section 3 describes the extreme precipitation analysis. Section 4 reports the changing precipitation pattern and large-scale teleconnections. Section 5 focuses on future climate projections and Section 6 summarizes the results.

2 | DATA SOURCES AND EXTREME PRECIPITATION DEFINITION

2.1 | Precipitation and river data

The daily precipitation data set used in this study is based upon the Asian Precipitation-Highly Resolved Observational Data Integration Towards Evaluation (APHRODITE) of the Water Resources project that covers the Asian monsoon domain (Yatagai *et al.*, 2012). We used a subset of the larger-domain APHRODITE data with a much-finer horizontal resolution ($0.05^\circ \times 0.05^\circ$) than the main set ($0.25^\circ \times 0.25^\circ$). This higher-resolution subset of APHRODITE data considered all available (more than 200) rainfall stations across Nepal, providing a more detailed spatial distribution of precipitation over mountainous regions than its 0.25° counterpart. Most of the global precipitation products (e.g., Global Precipitation Climatology Center, Global Precipitation Climatology Project, and so on) underestimate the precipitation over the Himalayan region (Yatagai *et al.*, 2012) even though station-based data are used to develop these products. APHRODITE data considered available precipitation station data, applied weighting scheme that considers the presence of a ridge between a rain gauge and a target cell, the presence of inclined slopes, adopted mountain mapping, and other procedure to obtain an observation data set as realistic as possible. Yatagai *et al.* (2012) compared the APHRODITE data to other precipitation dataset and show a significant improvement in

APHRODITE data compared with other products, especially in heavy rainfall. We do caution the limitation of measurements in high-mountain Nepal, since only 7–18% of the precipitation stations are located in high mountains (>2000 m) that cover nearly half of the total area of Nepal (Talchabhadel and Karki, 2019). However, the high-resolution APHRODITE data set is only available from 1951 to 2007, omitting the most recent decade. Due to potential reliability issues in observations prior to 1960, this study further parsed APHRODITE to only include post-1961 data for the extreme precipitation analysis. For the interannual variability analysis, the full period (1951–2007) annual and seasonal precipitation was used, since monthly APHRODITE data are comparable with other coarser-resolution datasets (results not shown).

To validate the observed changes in precipitation, we also examined historical hydrological data of river flow collected from the Department of Hydrology and Meteorology, Government of Nepal. To corroborate precipitation trends (discussed later), attention was placed on rivers in three regions across Nepal; the Karnali River (western), the Bagmati River (central), and the Koshi River (eastern). Hydrological data representing the maximum and minimum annual stream flow of these rivers are considered between 1981 and 2007. Dry season (minimum) flow typically occurs either in March or April while peak (maximum) flow is measured during July or August during monsoon season. We note that Koshi River data was only available from 1982 and all three rivers contained one or two periodic missing years. The Karnali River, which drains most parts of western Nepal should reflect the decreasing precipitation trends in western Nepal, while the Bagmati River basin draining south-central Nepal should reflect precipitation increases. With mixed precipitation trends, eastern Nepal's Koshi River basin should provide some guidance on how precipitation is affecting water resources.

2.2 | Climate data

To assess the future of precipitation, we used the Coupled Model Inter-comparison Project phase 5 (CMIP5; Taylor *et al.*, 2012), obtained from <http://climexp.knmi.nl/>. Each model of CMIP5 was driven with historical forcing (observation of aerosols, greenhouse gases, and solar irradiance) from 1910 to 2005, with 2006–2,100 following the representative concentration pathway 8.5 (RCP8.5) (Freychet *et al.*, 2015). We used 87 ensembles from 30 Global Climate models of CMIP5 historical precipitation data and 52 ensembles from 28 models for RCP8.5 future data (<http://climexp.knmi.nl/>). To capture the

east–west divide shown in observations, we split the CMIP5 annual precipitation along the 84°E meridian. We did not apply any bias correction in CMIP5 data since the model uncertainty is large and resolution is much coarser, so we had to examine the simulated precipitation time series independently.

To assess the regional teleconnections between ocean conditions and precipitation patterns, monthly sea surface temperature (SST) data were derived from the National Oceanic and Atmospheric Administration (NOAA)'s extended reconstructed SST [ERSST, version 4; Huang *et al.*, 2015]. We also utilized NCEP/NCAR reanalysis R1 data (Kalnay *et al.*, 1996) to resolve global-scale atmospheric circulation.

2.3 | Extreme precipitation definition

Extreme precipitation events are common during the Indian monsoon; however, parts of Nepal have seen an increase in the frequency and magnitude of extreme events in recent years (Karki *et al.*, 2017; Talchabhadel *et al.*, 2018). In the previous studies that computed the extreme precipitation statistics (e.g., Baidya *et al.*, 2008; Karki *et al.*, 2017; Talchabhadel *et al.*, 2018) and conducted case studies (Houze *et al.*, 2007; Romatschke *et al.*, 2010; Romatschke and Houze, 2011), a broad range of thresholds was used for the definition of extreme precipitation events; most of those were derived specifically for the Indian monsoon region. Given Nepal's broad range of precipitation variability (Ichiyangi *et al.*, 2007), the use of a fixed threshold like those shown in Talchabhadel *et al.* (2018) may not be appropriate to classify extreme precipitation events, a trait that has been documented (Haylock and Nicholls, 2000; Manton *et al.*, 2001; Goswami *et al.*, 2006; Pai *et al.*, 2015). To account for the series of extreme precipitation across Nepal, we used a bin approach with bins ranging between 50 and 300 mm/day with 50 mm intervals (bin size) to quantify the distribution of extreme precipitation.

First, for each daily time step between the summer monsoon season (June–September), we calculated the total number of grid points ($0.05^\circ \times 0.05^\circ$ resolution) that contain daily precipitation intensity greater than the given threshold. By summing these daily occurrences over the entire season relative to the total number of daily grid points possible, we established the seasonal frequency of extreme precipitation occurred in both space and time for that year. We defined these as the *spatial frequency*. Second, we partitioned the *spatial frequency* for each precipitation intensity threshold into decadal intervals. Finally, we normalized each intensity threshold's decadal intervals by the full-period frequency (decadal

frequency/total frequency) from 1961 to 2007. The normalized frequency for each precipitation intensity threshold was converted into a percentage and referred to as *normalized extreme precipitation frequency (%)*. The detail of the frequency calculation method with mathematical equation is provided in supplementary material. We note that the last group of decadal frequencies (2001–2007) contained only 7 years of data; in order to preserve consistency, this period was converted into a 10-year frequency.

3 | DISTRIBUTION OF EXTREME PRECIPITATION

3.1 | Extreme precipitation statistics and change

Figure 2 shows the normalized daily precipitation extremes in each threshold accumulated in western and eastern Nepal at the decadal interval. Both regions experienced extreme precipitation events during the last 5 decades. However, western Nepal experienced more extreme events during the earlier period (Figure 2a) and revealed some interdecadal variability, while eastern Nepal shows a different distribution of extreme precipitation (Figure 2b). Extreme precipitation during the early decades (the 1960s to 1970s) resembles dominant lower-intensity precipitation events (>50, 100, and 150 mm/day). During the 1980's, all extreme precipitation intensity categories experienced an increase compared with the previous two decades, while the greatest increases occurred within the 100 and 200 mm/day range. During the 1990's, precipitation continued to shift towards more extreme events with roughly a doubling of daily precipitation >300 mm/day. This finding coincides with those found over central India (Roxy *et al.*, 2017). Even though recent extreme precipitation studies (Bohlinger and Sor-teberg, 2017; Karki *et al.*, 2017; Talchabhadel *et al.*, 2018) show both increasing and decreasing trends in different parts of Nepal, these studies only utilized the fixed maximum precipitation value or station-based, 1-day maximum precipitation to represent the trend. In comparison, by using the total number of grid points and the frequency of precipitation intensity across a broad range of intervals in eastern Nepal, we have identified the reversal in extreme precipitation distribution that occurred in 2001–2007 (shown by the red arrows in Figure 2b); this is a previously undocumented feature.

We further diagnosed the extreme precipitation frequency in different topographical regions. By considering five topographical regions based on elevation (above mean sea level), lower than 1,000 m, between 1,000 and

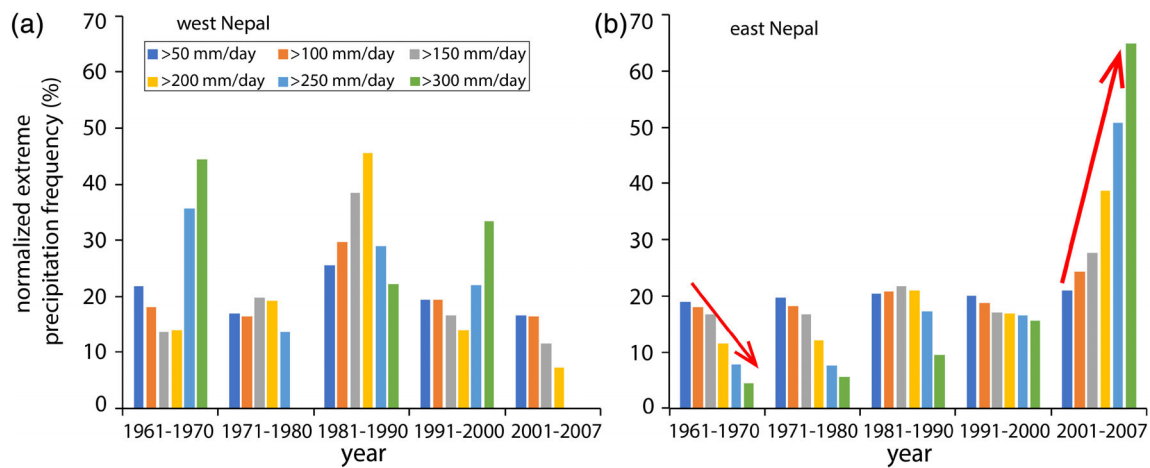


FIGURE 2 Normalized extreme precipitation frequency distribution in percentage for precipitation intensity larger than 50 mm/day to larger than 300 mm/day considering every 50 mm interval range for western (left panel) and eastern (right panel) Nepal. The frequency is calculated as the total grid points for the given intensity of precipitation every year and calculated total grid points for every 10 years period. The 10 years grid points are normalized (divided by the total grid points from 1961 to 2007) for each interval for given intensity of precipitation and calculated the percentage. Red arrows in right panel show the direction of extreme precipitation frequency distribution [Colour figure can be viewed at wileyonlinelibrary.com]

2000 m, between 2000 and 3,000 m, between 3,000 and 4,000 m, and above 4,000 m for the extreme precipitation frequency analysis, the results are shown in Figure 3. The whole-Nepal analysis considering all elevations (Figure 3a) shows a similar result with eastern Nepal (Figure 2b), indicating that higher intensity (>200–300 mm/day) extreme precipitation events have increased dramatically in recent years. The distribution extreme for the lower elevation (<1,000 m, Figure 3b) reveals the same distribution as for whole Nepal. The highest intensity (>300 mm/day) precipitation extremes between 1,000 and 3,000 m elevation regions (Figure 3c, d) was not common in earlier years (before 2000), but started to appear more frequently since the early 21st century. Higher intensity (>200 mm/day) extreme events are very uncommon over higher elevations (higher than 3,000 m, Figure 3e,f) and lower intensity precipitation does not show any change in distribution during the last five decades.

3.2 | Impact on stream flow

The decreasing precipitation in western Nepal is also observed before 1981, albeit with a less pronounced east-west contrast. To evaluate the impact of precipitation change, three rivers are considered. Western Nepal is home to the Karnali River; the longest river in Nepal. Khatiwada *et al.* (2016) conducted a hydroclimatic study of the Karnali basin and showed significant temperature increases, but they did not examine the dry season flow. To supplement the results that annual precipitation has

decreased in the region, we first examined the precipitation and stream flow from the post-monsoon months (October to February). First, precipitation during these months shows a similar trend (results not shown) that corresponds to the annual precipitation (Figure 1a). The dry-season flow of the Karnali River also reveals a decreasing trend (Figure 1c) while annual maximum flow does not show significant change (Figure 1b) in response to the precipitation decrease. Since western Nepal is historically a drought-prone region, the decreasing precipitation and associated reduction in stream flow indicates an increase in drought risk to the region's water shortages since 2008 (Wang *et al.*, 2013). Such a scenario has wide-ranging implications for the region's ability to secure water resources for irrigation and hydropower.

Focusing on southcentral Nepal's Bagmati River, the increasing precipitation trend resulted in a corresponding increase to stream flow (Figure 1d,e). This region also experienced an increase in extreme precipitation, which translated to a compound increase in the maximum flow. Consistent with the mixed precipitation trends throughout eastern Nepal, the Koshi River flow does not show any noticeable trend to either dry season or maximum flow (Figure 1f,g).

3.3 | Longer-term variability

The spatial distribution of moderate to high intensity precipitation trend (Figure 4) shows that most of the extreme precipitation occurred in the southern part of Nepal where orographic lifting along the Churia mountain

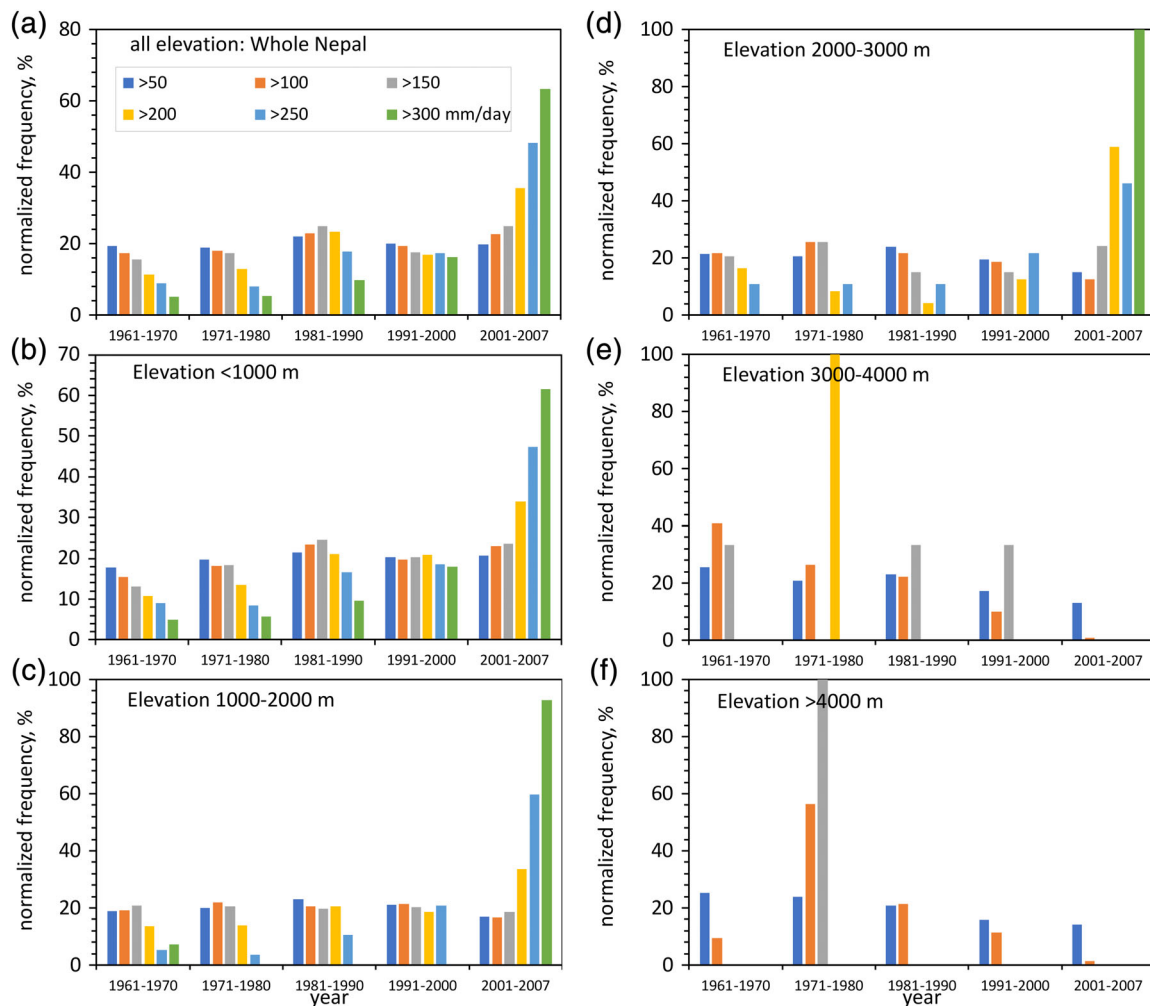


FIGURE 3 Normalized extreme precipitation frequency distribution in percentage for precipitation intensity larger than 50 mm/day to larger than 300 mm/day considering every 50 mm interval range for whole Nepal at different altitude regions. (a) is for whole Nepal considering all elevation, (b) is from elevation less than 1,000 m, (c) is from 1,000 to 2000 m elevation, (d) is from 2000 to 3,000 m elevation, (e) is from 3,000 to 4,000 m elevation, and (f) from elevation higher than 4,000 m regions. Colour bar represents the different intensity of precipitation rate (given in first panel) [Colour figure can be viewed at wileyonlinelibrary.com]

range (green dashed line) deposits a significant amount of rainfall. Generally, seasonal precipitation decreases from the southern mountain ranges to the northern part of Nepal, with some of the highest rainfall areas located on the southern slope of the highest mountains (e.g., Dhar and Nandargi, 2005). The moderate precipitation (>100 mm/day) events show an increasing trend in most of the southern part of the country (Figure 4a), while heavy precipitation (>150 mm/day) events show increasing trend in eastern Nepal and over the south-central region. Western Nepal shows a mixed result (Figure 4b). Very heavy precipitation (>200, >250, and >300 mm/day) events only occurred in confined area of southcentral region and shows significant increases in recent years (not shown). The increasing trend to extreme precipitation in Nepal is consistent with Roxy *et al.* (2017); Pai *et al.* (2015); and Goswami *et al.* (2006),

which also reveal the increasing extreme precipitation frequency over the northern and central India. The result presented here adds further details to these previous studies, especially the accelerated increase in the more-extreme precipitation in the recent decade and the east-west division of the precipitation pattern.

4 | DRIVERS OF THE CHANGING PRECIPITATION

To explore the temporal variations of the aforementioned precipitation patterns in Nepal, we applied the Empirical Orthogonal Functions (EOFs) analysis on annual precipitation anomaly during 1951–2007. EOF analysis of precipitation provides the spatial modes/patterns of variability and how they change with time (Hannachi,

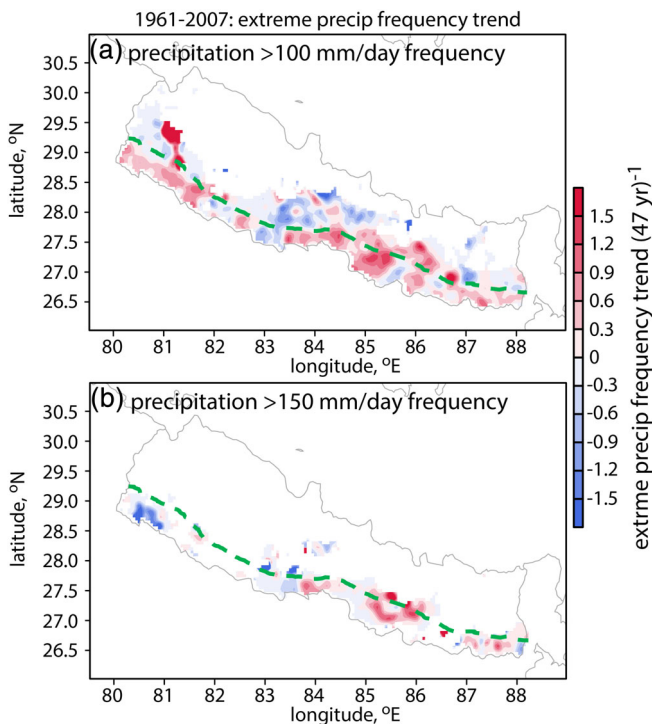


FIGURE 4 Extreme precipitation frequency trend from 1961 to 2007 (in 47 years) for precipitation intensity (a) larger than 100 mm/day and (b) larger than 150 mm/day. Dashed green lines in both panel shows the location of Churia range just north of southern plain area [Colour figure can be viewed at wileyonlinelibrary.com]

2004; Monahan *et al.*, 2009). Since the first two modes and corresponding principal components (PCs) account for about 50% of the variance explained, we only considered this pair for discussion. The first mode represents the majority of the variance (35%; Figure 5a), which displays the broad monsoonal precipitation variability that is connected to the Indian summer monsoon (Wang and Gillies, 2013). The second mode (EOF2) of annual precipitation, which displays 13% of variability (Figure 5b), displays the east–west division corresponding to the long-term trend pattern (Figure 1a). If the principle component of second mode (PC2) positive phase occurs in the first mode (PC1) neutral phase, then the net effect would be predominantly PC2. Indeed, the PC2 shows an increasing trend, suggesting that precipitation in western Nepal has been decreasing. Although not shown, this pattern was present throughout all seasons. This suggests a rather uniform annual precipitation reduction in western Nepal throughout 1951–2007 with more significant decrease after 1981. We further investigate the seasonal precipitation trend (figure not shown) and observed the east west division on precipitation trend during all season. However, winter and pre-monsoon seasons experienced relatively larger decrease of precipitation in western Nepal relative to monsoon and postmonsoon seasons. Eastern Nepal, mainly southcentral Nepal reveals largest increase in precipitation trend during monsoon season. Further examination of the Indian

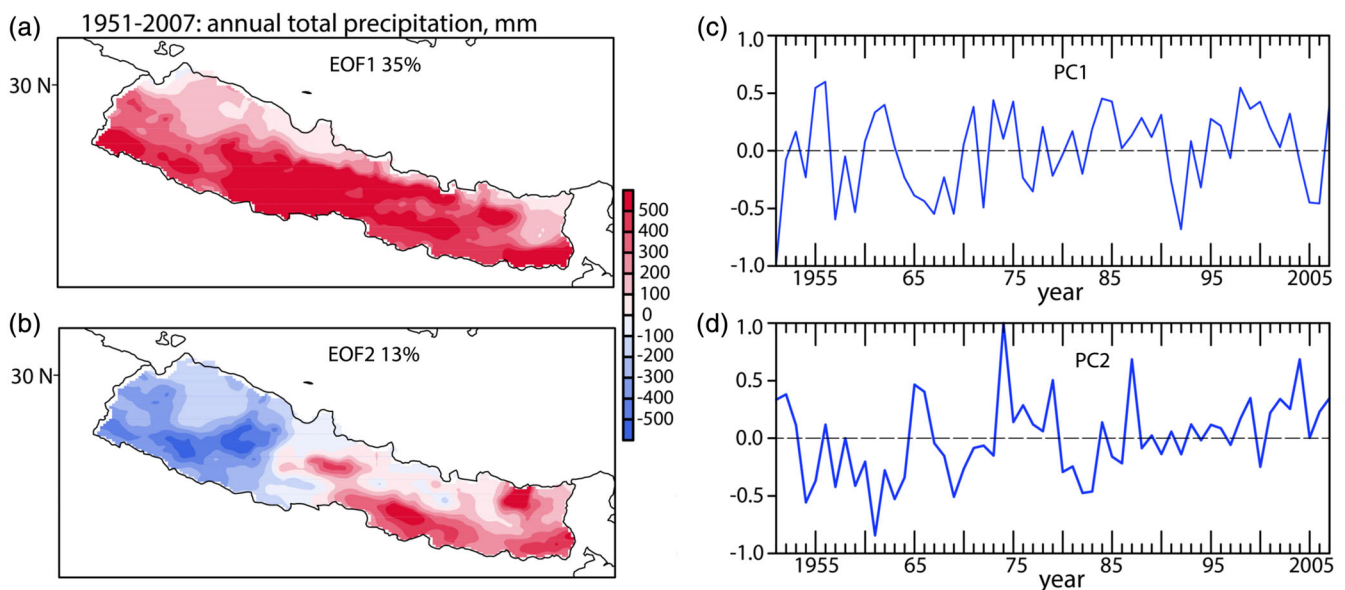


FIGURE 5 First two modes of Empirical orthogonal function (EOF) of total annual precipitation of Nepal from 1951 to 2007. (a) EOF1 with 35% variance, (b) EOF2 with 13% variance, (c) principal component (PC) of first mode, and (d) PC of second mode [Colour figure can be viewed at wileyonlinelibrary.com]

Summer Monsoon (ISM) index found that the ISM index is decreasing during the same period (1951–2007) and that the increasing trend of PC2 was negatively correlated with the ISM index (Figure S1).

To investigate whether oceanic forcing plays a role in these precipitation changes, we compare the precipitation PC time series against the SST anomalies worldwide. To focus on interannual variability, we removed the linear trend of the PCs and correlated them with the detrended annual-mean SST; the results are shown in Figure 6. PC1 is highly correlated with an apparent La Nina pattern with a broad cold-SST anomaly over tropical eastern Pacific and warmer SST in the western Pacific (Figure 6a), reflecting the well-known role of the El Nino-Southern Oscillation as a driver of the Indian summer monsoon. The SST correlations with PC2, that is, the east–west division in precipitation anomalies, are only significant in the southern Indian ocean (Figure 6b). Opposite SST correlations between PC1 and PC2 are

observed over the northwest coast of Australia. These features and the lack of broad-scale SST correspondence in PC2 suggest that this second leading mode of precipitation variability in Nepal (i.e., the east–west division) is likely driven by atmospheric variability and possibly modulated by the Indian Ocean (Ding and Wang, 2005). Analysing Nepal's summer monsoon, Wang *et al.* (2013) reported that the decadal-scale precipitation variation corresponds to the transition between El Nino and La Nina phases, which lends support to the largely insignificant SST correlations in Figure 6b with respect to the apparent low-frequency variability in PC2. Since the Indian Ocean is warming at a steady rate (Roxy *et al.*, 2014), the decreasing precipitation trend in western Nepal may not persist in the future as the warming Indian Ocean overcomes the interannual cold anomaly.

Nepal lies at the northern periphery of the Indian Monsoon where the Himalayan mountains located just to the north block the moisture-laden monsoonal winds

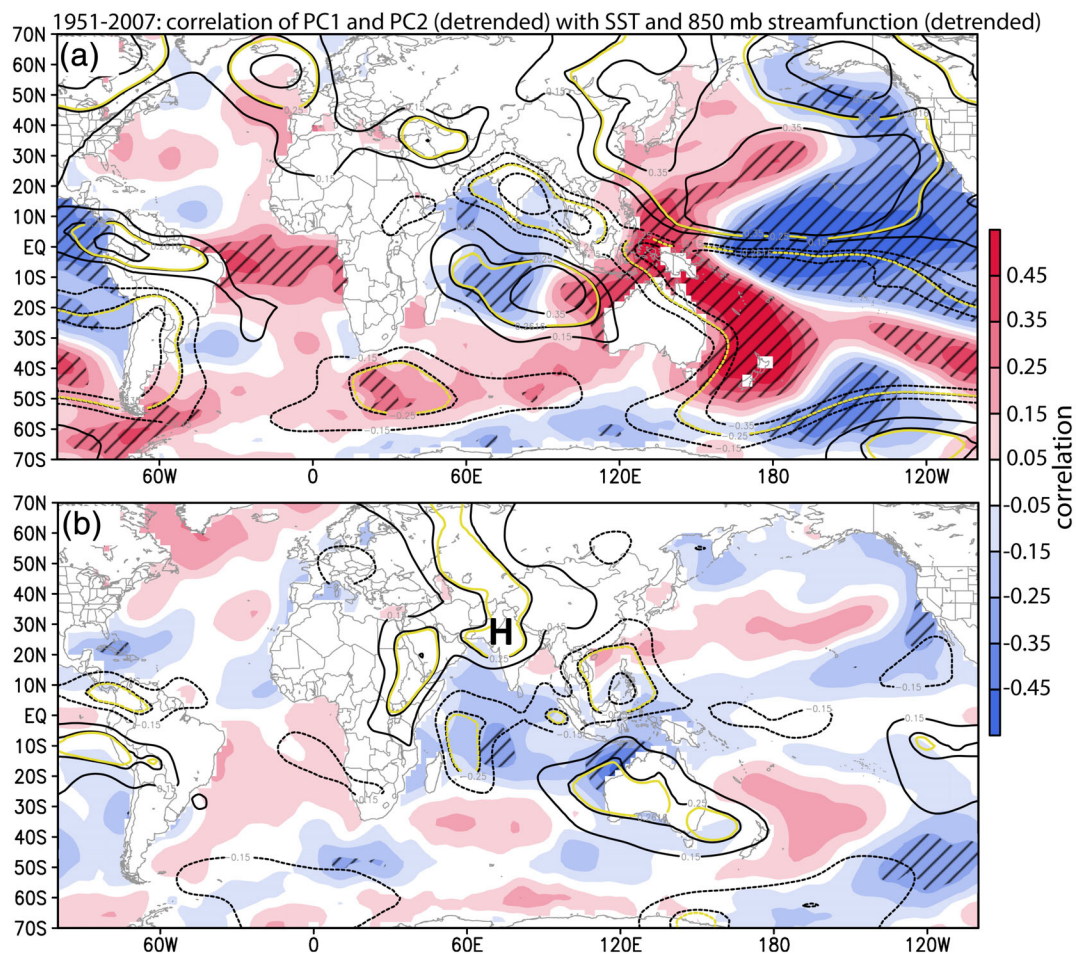


FIGURE 6 Temporal correlation of annual precipitation principal component (PC) to annual SST (colour filled) and to 850 mb streamfunction (contour) after removing the trend of PC, SST, and height) from 1951 to 2007. (a) PC1 correlation with SST and height and (b) PC2 correlation with SST and height. Hatched areas indicate that significant values with $p < .05$ with SST and yellow contours show significant values with $p < .05$ with stream function [Colour figure can be viewed at wileyonlinelibrary.com]

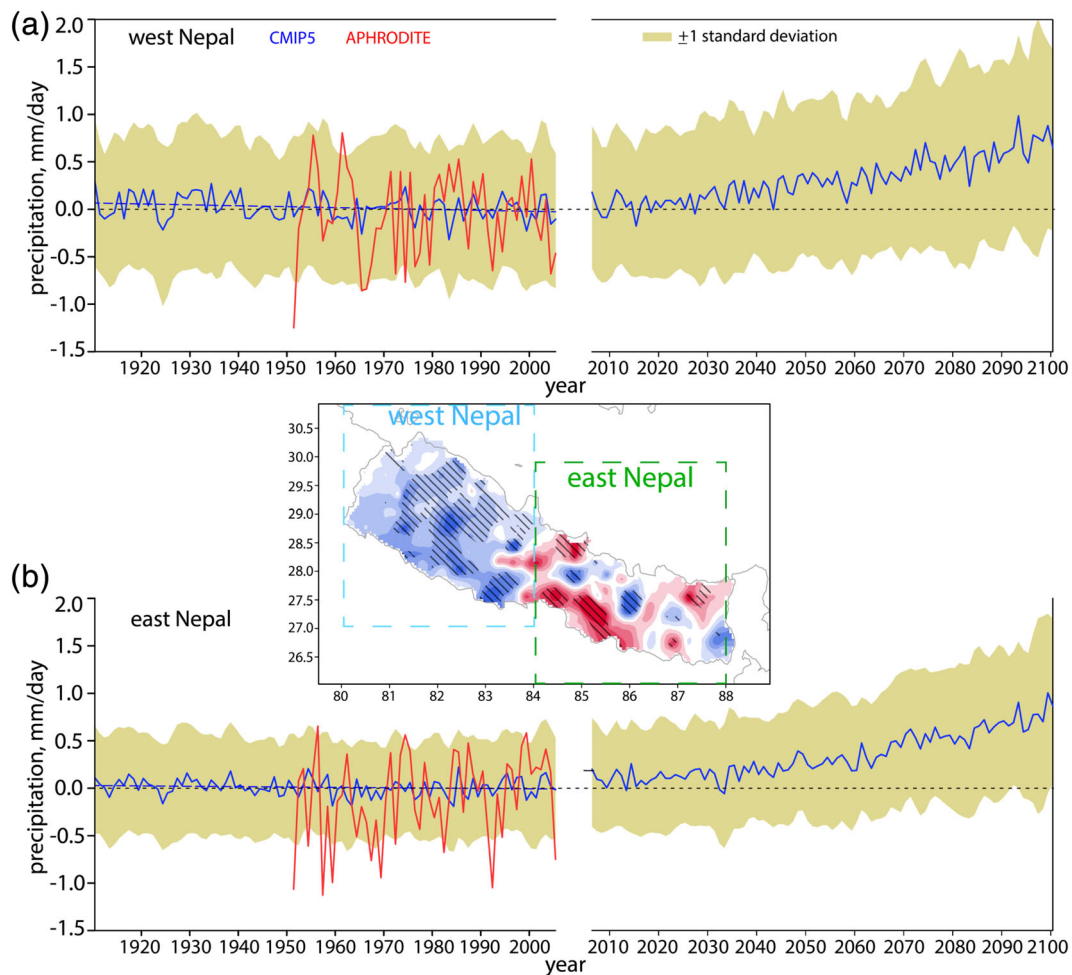


FIGURE 7 CMIP5 annual precipitation anomaly (mm/day, blue line) from 1910 to 2005 for historical period and from 2006 to 2,100 for RCP8.5 scenario considering (a) western Nepal and (b) eastern Nepal. The domain of the two region is shown in inserted map. The anomaly is calculated based on 1971–2000 average precipitation for individual CMIP5 ensemble member and shaded area is the ± 1 SD of average value. Average and SD are calculated considering all members for each year from 1910 to 2,100 (87 ensembles from 30 models for historical and 50 ensembles from 20 models for RCP8.5 future scenario are considered in this analysis. Red line is from high-resolution APHRODITE data. Black and blue dashed lines in (a) and (b) show 0 line and linear trend of CMIP data, respectively [Colour figure can be viewed at wileyonlinelibrary.com]

from penetrating further inland (Choudhury and Krishnan, 2011; Turner and Annamali, 2012). The monsoon moisture that contributes most to the annual precipitation enters first throughout eastern Nepal before eventually moving towards western Nepal (Ichiyanagi *et al.*, 2007; Talchabhadel *et al.*, 2018). In this regard, the PC1 correlates with the low level (850 mb) streamfunction (contours in Figure 6a) that shows positive correlation over the Indian ocean and negative correlation over Indian subcontinent. However, the PC2 shows significant positive correlation over western Nepal (yellow solid line Figure 6b), while negatively correlated over Indian Ocean indicating opposite correlation than the PC1. This indicates high pressure over western Nepal and increasing dry and cold air coming from Tibetan Plateau associated with the decreasing precipitation,

whereas eastern Nepal receives warmer and moist air from the Bay of Bengal that may have helped the increase in precipitation.

5 | CLIMATE PROJECTION OF PRECIPITATION

To assess future change to precipitation extremes with respect to the observed changes, we next analysed the climate model projections of CMIP5. We considered the annual average of precipitation from multi-model ensembles over the western and eastern Nepal. Precipitation anomaly was calculated based on the 1971–2000 average for individual ensemble members, and SD and average were calculated by considering all members from 1910 to

2,100. Next, we separated precipitation in western and eastern Nepal regions using 84°E as the boundary (inset of Figure 7). The average precipitation anomaly from historical CMIP5 simulations and future projections based on the RCP8.5 scenario is shown in Figure 7. The multi-model mean of the CMIP5 shows reasonable spatial distribution of precipitation over the South Asian monsoon region, even though inter-model spread remains large and the dry bias in monsoon rainfall is present in many models (Sperber *et al.*, 2013; Freychet *et al.*, 2015; Hagos *et al.*, 2019).

CMIP5 models capture the large year-to-year variability in eastern and western Nepal; however, when compared with observations, the variability is noticeably smaller (Figure 7). One other noticeable point of deviation from observations is the greater variability CMIP5 members produced for western Nepal (Figure 7a) compared with eastern Nepal (Figure 7b), whereas observations are comparable across regions. Interestingly, the historical CMIP5 precipitation shows decreasing trend in western Nepal (blue dashed line in Figure 7a) for the 1861–2005 period, with a 99% confidence interval, but does not show any significant trend in eastern Nepal. Even though both historical climate model data and observation agree that western Nepal's precipitation is decreasing, the result should be interpreted with caution as the period of record and the horizontal resolution are different between the two data sets.

Consistent with Kadel *et al.* (2018) and Krishnan *et al.* (2019), the RCP8.5 climate model ensemble projects increasing precipitation trends in both eastern and western Nepal (Figure 7). As mentioned in Section 5, the decreasing trend of precipitation in western Nepal could potentially be mitigated by the ongoing warming of the Indian Ocean and the Indian subcontinent (Jin and Wang, 2017), as well as the accelerated warming in the Hindu Kush Himalayan region (Krishnan *et al.*, 2019). Jin and Wang (2017) showed that the Indian summer monsoon precipitation was decreasing until 2002, at which point the trend reversed towards increasing precipitation. The increasing trend of future precipitation becomes faster after the mid-21st century in both regions, despite the pronounced model uncertainty for western Nepal's precipitation projection. Comparisons between RCP2.6, RCP4.5, and RCP8.5 indicated similar precipitation trends in the future with increasing variation in precipitation with more aggressive RCP scenario.

We further looked the seasonal precipitation projection under RCP8.5 scenario over western and eastern Nepal (result not shown) and found that the monsoon and post-monsoon precipitation will increase continuously in both regions. However, winter precipitation will decrease in both reason and pre-monsoon precipitation

will decrease in western Nepal, while eastern Nepal does not experience a significant change during pre-monsoon. Since annual precipitation will increase while winter precipitation decreases in both regions, the intensity of precipitation may increase in the future warming climate.

We should note that Nepal's increasing precipitation trend predicted under a future warming climate is different from the precipitation trend projected for the larger region of Hindu-Kush-Himalayan region discussed by Palazzi *et al.* (2013). Palazzi *et al.* (2013) described an increasing precipitation trend until the middle of the century (2050). However, when refining the study area to the smaller Nepal-only domain, the increasing trend is predicted to extend until the end of 21st century. Moreover, Sandeep *et al.* (2018) showed that a warming climate will promote the activity of low-pressure systems that will bring more extreme precipitation events to northern India and Nepal.

6 | SUMMARY AND CONCLUSIONS

Precipitation in the Himalayan region is highly variable in both space and time with some of the most extreme amounts on the planet. This study expands on previous studies investigating extreme precipitation by documenting the changing pattern of precipitation in Nepal using a high-resolution ($0.05^{\circ} \times 0.05^{\circ}$) subset of the APH-RODITE daily precipitation dataset up to 2007. In general, this study identified an east–west division in the precipitation trends, with western Nepal experiencing a decrease of precipitation around 1981, while eastern Nepal experienced an increase in precipitation. Even though locations of the decreasing trend vary in different seasons, the east–west division of precipitation change persists through all four seasons (winter, pre-monsoon, monsoon, and post-monsoon). Corresponding to the decreasing precipitation throughout western Nepal, the dry-season flow of the region's primary river system is found to decrease as well; this finding implies negative impacts on the region's agriculture, ecosystems, and socio-economic security.

Given the highly variable nature of precipitation across the country, this study addressed the changes to extreme events via a set of thresholds, as opposed to a singular threshold commonly used by previous studies. In general, extreme events have become more common and increasingly extreme, with the expectation for this trend to continue as a warming climate brings elevated atmospheric humidity and greater precipitable water (Goswami *et al.*, 2006; Krishnan *et al.*, 2019). To identify the potential causes of the east–west division in

precipitation trends, this study depicted the region's interannual variability relationship with the Indian Ocean SST. As the Indian Ocean warms (Roxy *et al.*, 2015) and the Indian sub-continent warms (Jin and Wang, 2017), the east–west division of precipitation trend may be overtaken by an overall increase across Nepal, that is, a result implicated by CMIP5 future precipitation projections under RCP 8.5.

The results presented here showcase the dramatic change to precipitation extremes with varying geographic distribution across Nepal. However, the limitation of the APRODITE precipitation record that ends in 2007 negates the most recent decade of examination. Therefore, future work should account for the most recent data as well as a more capable model assessment utilizing higher-resolution or regional climate simulations. Specifically, an investigation into the regional climate modelling data such as that focused on the Indian subcontinent and Nepal, produced by the Coordinated Regional Climate Downscaling Experiment (CORDEX) project's downscaling efforts, is needed to verify the recent trends.

ACKNOWLEDGEMENTS

This research was supported by the U.S. Department of Energy grant DESC0016605 and the Utah State University Agricultural Experiment Station under paper 9251. We thank Department of Hydrology and Meteorology, Government of Nepal for the APHRODITE and river data. We would like to offer special thanks to Ramchandra Karki, who although no longer with us.

ORCID

Binod Pokharel  <https://orcid.org/0000-0002-6369-7525>

REFERENCES

- Adhikari, S. (2019) Drought impact and adaptation strategies in the min-hill farming system of Western Nepal. *Environments*, 5, 101. <https://doi.org/10.3390/environments5090101>.
- Baidya, S.K., Shrestha, M.L. and Sheikh, M.M. (2008) Trends in daily climatic extremes of temperature and precipitation in Nepal. *Journal of Hydrology and Meteorology*, 5(1), 38–51.
- Bohlinger, P. and Sorteberg, A. (2017) A comprehensive view on trends in extreme precipitation in Nepal and their spatial distribution. *International Journal of Climatology*. <https://doi.org/10.1002/joc.5299>.
- Bohlinger, P., Sorteberg, A., Liu, C., Rasmussen, R., Sodeman, H. and Ogawa, F. (2018) Multiscale characteristics of an extreme precipitation event over Nepal. *Quarterly Journal of the Royal Meteorological Society*, 145, 179–196. <https://doi.org/10.1002/qj.3418>.
- Choudhury, A.D. and Krishnan, R. (2011) Dynamical response of the South Asian monsoon trough to latent heating from stratiform and convection precipitation. *Journal of the Atmospheric Sciences*, 68, 1347–1363.
- Dhar, O.N. and Nandargi, S. (2005) Areas of heavy precipitation in the Nepalese Himalayas. *Weather*, 60(12), 354–356.
- Ding, Q. and Wang, B. (2005) Circumglobal teleconnection in the northern hemisphere summer. *International Journal of Climatology*, 18, 3483–3505.
- Freychet, N., Hsu, H.-H., Chou, C. and Wu, C.-H. (2015) Asian summer monsoon in CMIP5 projections: A link between the change in extreme precipitation and monsoon dynamics. *Journal of Climate*, 28, 1477–1493.
- Goswami, B.N., Venugopal, V., Sengupta, D., Madhusoodanan, M. S. and Xavier, P.K. (2006) Increasing trend of extreme rain events over India in a warming environment. *Science*, 314, 1442–1445.
- Houze, R.A., Wilton, D.C. and Smull, B.F. (2007) Monsoon convection in the Himalayan region as seen by the TRMM precipitation radar. *Quarterly Journal of the Royal Meteorological Society*, 133(627), 1389–1411. <https://doi.org/10.1002/qj.106>.
- Hannachi, A. (2004) *A Primer for EOF Analysis of Climate Data*. Reading, UK: Department of Meteorology, University of Reading, p. 33.
- Haylock, M. and Nicholls, N. (2000) Trends in extreme rainfall indices for an updated high quality data set for Australia, 1910–1998. *International Journal of Climatology*, 20, 1533–1541.
- Hagos, S., Leung, L.R., Ashfaq, M. and Balaguru, K. (2019) South Asian monsoon precipitation in CMIP5: A link between inter-model spread and the representations of tropical convection. *Climate Dynamics*, 52, 1049–1061.
- Huang, B., Banzon, V.F., Freeman, E., Lawrimore, J., Liu, W., Peterson, T.C., Smith, T.M., Thorne, P.W., Woodruff, S.D. and Zhang, H.M. (2015) Extended reconstructed sea surface temperature Version 4 (ERSST.v4). Part I: Upgrades and Intercomparisons. *Journal of Climate*, 28, 911–930.
- Ichiyanagi, K., Yamanaka, M.D., Muraji, Y. and Vaidya, B.K. (2007) Precipitation in Nepal between 1987 and 1996. *International Journal of Climatology*, 27, 1753–1762.
- Jin, Q. and Wang, C. (2017) A revival of Indian summer monsoon rainfall since 2002. *Nature Climate Change*, 7, 587–594. <https://doi.org/10.1038/NCLIMATE3348>.
- Kalnay, E., Kanamitsu, M., Kistler, R., Collins, W., Deaven, D., Gandin, L., Iredell, M., Saha, S., White, G., Woollen, J., Zhu, Y., Leetmaa, A., Reynolds, R., Chelliah, M., Ebisuzaki, W., Higgins, W., Janowiak, J., Mo, K.C., Ropelewski, C., Wang, J., Jenne, R. and Joseph, D. (1996) The NCEP/NCAR 40-year reanalysis project. *Bulletin of the American Meteorological Society*, 77, 437–471.
- Krishnan, R., Shrestha, A.B., Ren, G., Rajbhandari, R., Saeed, S., Sanjay, J., Syed, M.A., Vellore, R., Xu, Y., You, Q. and Ren, Y. (2019) Unravelling climate change in the Hindu Kush Himalaya: rapid warming in the mountains and increasing extremes. In: Wester, P., Mishra, A., Mukherji, A. and Shrestha, A. (Eds.) *The Hindu Kush Himalaya Assessment*. Cham, Germany: Springer.
- Kadel, I., Yamazaki, T., Iwasaki, T. and Abdillah, M.R. (2018) Projection of future monsoon precipitation over the Central Himalayas by CMIP5 models under warming scenario. *Climate Research*, 75, 1–21.
- Kansakar, S.R., Hannah, D.M., Gerrard, J. and Rees, G. (2004) Spatial pattern in the precipitation regime in Nepal. *International*

- Journal of Climatology*, 24(13), 1645–1659. <https://doi.org/10.1002/joc.1098>.
- Karki, R., Hasson, S., Schickhoff, U., Scholten, T. and Bohner, J. (2017) Rising precipitation extremes across Nepal. *Journal of Climate*, 5, 4. <https://doi.org/10.3390/cli5010004>.
- Khatiwada, K., Panthi, J., Shrestha, M. and Nepal, S. (2016) Hydro-climatic variability in the Karnali River basin of Nepal Himalaya. *Climate*, 4(2), 17. <https://doi.org/10.3390/cli4020017>.
- Manton, M.J., Della-Marta, P.M., Haylock, M.R., Hennessy, K.J., Nicholls, N., Chambers, L.E., Collins, D.A., Daw, G., Finet, A., Gunawan, D., Inape, K., Isobe, H., Kestin, T.S., Lefale, P., Leyu, C.H., Lwin, T., Maitrepierre, L., Ouprasitwong, N., Page, C.M., Pahalad, J., Plummer, N., Salinger, M.J., Suppiah, R., Tran, V.L., Trewin, B., Tibig, I. and Yee, D. (2001) Trends in extreme daily rainfall and temperature in Southeast Asia and the South Pacific: 1961–1998. *International Journal of Climatology*, 21, 269–284.
- Monahan, A., Fyfe, J.C., Ambaum, M.H., Stephenson, D.B. and North, G.R. (2009) Empirical orthogonal functions: The medium is the message. *Journal of Climate*, 22, 6501–6514.
- Pai, D., Sridhar, L., Badwaik, M. and Rajeevan, M. (2015) Analysis of the daily rainfall events over India using a new long period (1901–2010) high resolution (0.25 × 0.25) gridded rainfall data set. *Climate Dynamics*, 45, 755–776.
- Palazzi, E., von Hardenberg, J. and Provenzale, A. (2013) Precipitation in the Hindu-Kush Karakoram Himalaya: Observations and future scenarios. *Journal of Geophysical Research: Atmosphere*, 118, 85–100. <https://doi.org/10.1029/2012JD018697> 2013.
- Romatschke, U. and Houze, R.A. (2011) Characteristics of precipitating convective systems in the South Asian monsoon. *Journal of Hydrometeorology*, 12(1), 3–26. <https://doi.org/10.1175/2010JHM1289.1>.
- Romatschke, U., Medina, S. and Houze, R.A. (2010) Regional, seasonal, and diurnal variations of extreme convection in the South Asian region. *Journal of Climate*, 23(2), 419–439. <https://doi.org/10.1175/2009JCLI3140.1>.
- Roxy, M.K., Ritiak, K., Terray, P. and Masson, S. (2014) The curious case of Indian Ocean warming. *Journal of Climate*, 27, 8501–8509.
- Roxy, M.K., Ritiak, K., Terray, P., Murtugudde, R., Ashok, K. and Goswami, B.N. (2015) Drying of Indian subcontinent by rapid Indian Ocean warming and a weakening land-sea thermal gradient. *Nature Communications*, 6. <https://doi.org/10.1038/ncomms8423>.
- Roxy, M.K., Ghosh, S., Pathak, A., Athulya, R., Mujumber, M., Murtugudde, R., Terray, P. and Rajeevan, M. (2017) A threefold rise in widespread extreme rain events over Central India. *Nature Communications*, 8, 708.
- Sandeep, S., Ajayamohan, R.S., Boos, W.R., Sabin, T.P. and Praveen, V. (2018) Decline and poleward shift in Indian summer monsoon synoptic activity in a warming climate. *Proceedings of the National Academy of Sciences*, 115, 2681–2686. <https://doi.org/10.1073/pnas.1709031115>.
- Sperber, K.R., Annamalai, H., Kang, I.-S., Kitoh, A., Moise, A., Turner, A., Wang, B. and Zhou, T. (2013) The Asian summer monsoon: An intercomparison of CMIP5 vs. CMIP3 simulations of the late 20th century. *Climate Dynamics*, 41, 2711–2744.
- Sudmeier-Rieux, K., Gaillard, J.C. and Sharma, S. (2012) Nepal: Landslides, Flooding and Adaptation Responses. In: Lamadrid, A. and Kelman, I. (Eds.) *Emerald Books Volume on Climate Change Modeling for Local Adaptation in the Hindu Kush-Himalayan Region*. Oslo, Norway: Center for International Climate and Environmental Research—Oslo (CICERO).
- Talchabhadel, R. and Karki, R. (2019) Assessing climate boundary shifting under climate change scenarios across Nepal. *Environmental Monitoring and Assessment*, 191(520), 520.
- Talchabhadel, R., Karki, R., Thapa, B.R., Maharjan, M. and Parajuli, B. (2018) Spatio-temporal variability of extreme precipitation in Nepal. *International Journal of Climatology*, 38, 4296–4313.
- Taylor, K.E., Stouffer, R.J. and Meehl, G.A. (2012) An overview of CMIP5 and the experiment design. *Bulletin of the American Meteorological Society*, 93, 485–498.
- Turner, A.G. and Annamali, H. (2012) Climate change and the South Asian summer monsoon. *Nature Climate Change*, 2, 587–595.
- Viste, E. and Sorteberg, A. (2015) Snowfall in the Himalayas: An uncertain future from a little-known past. *The Cryosphere*, 9, 1147–1167.
- Wang, S.-Y. and Gillies, R.R. (2013) Influence of the Pacific quasi-decadal oscillation on the monsoon precipitation in Nepal. *Climate Dynamics*, 40, 95–107.
- Wang, S.Y., Yoon, J.H., Gillies, R.R. and Cho, C. (2013) What caused the winter drought in western Nepal during recent years? *Journal of Climate*, 26, 8241–8256.
- Yatagai, A., Kamiguchi, K., Arakawa, O., Hamada, A., Yasutomi, N. and Kitoh, A. (2012) APHRODITE: Constructing a long-term daily gridded precipitation dataset for Asia based on a dense network of rain gauges. *Bulletin of the American Meteorological Society*, 93, 1401–1415.

SUPPORTING INFORMATION

Additional supporting information may be found online in the Supporting Information section at the end of this article.

How to cite this article: Pokharel B, Wang S-YS, Meyer J, *et al.* The east–west division of changing precipitation in Nepal. *Int J Climatol.* 2020;40: 3348–3359. <https://doi.org/10.1002/joc.6401>